

# Loss of the Transit Peptide and an Increase in Gene Expression of an Ancestral Chloroplastic Carbonic Anhydrase Were Instrumental in the Evolution of the Cytosolic C<sub>4</sub> Carbonic Anhydrase in *Flaveria*<sup>1[CI][OA]</sup>

Sandra K. Tanz<sup>2</sup>, Sasha G. Tetu<sup>3</sup>, Nicole G.F. Vella, and Martha Ludwig\*

Department of Biological Sciences, Macquarie University, Sydney, New South Wales 2109, Australia (S.K.T., S.G.T., N.G.F.V.); and School of Biomedical, Biomolecular, and Chemical Sciences, University of Western Australia, Crawley, Western Australia 6009, Australia (M.L.)

C<sub>4</sub> photosynthesis has evolved multiple times from ancestral C<sub>3</sub> species. Carbonic anhydrase (CA) catalyzes the reversible hydration of CO<sub>2</sub> and is involved in both C<sub>3</sub> and C<sub>4</sub> photosynthesis; however, its roles and the intercellular and intracellular locations of the majority of its activity differ between C<sub>3</sub> and C<sub>4</sub> plants. To understand the molecular changes underlying the evolution of the C<sub>4</sub> pathway, three cDNAs encoding distinct  $\beta$ -CAs (CA1, CA2, and CA3) were isolated from the leaves of the C<sub>3</sub> plant *Flaveria pringlei*. The phylogenetic relationship of the *F. pringlei* proteins with other embryophyte  $\beta$ -CAs was reconstructed. Gene expression and protein localization patterns showed that CA1 and CA3 demonstrate high expression in leaves and their products localize to the chloroplast, while CA2 expression is low in all organs examined and encodes a cytosolic enzyme. The roles of the *F. pringlei* enzymes were considered in light of these results, other angiosperm  $\beta$ -CAs, and *Arabidopsis* (*Arabidopsis thaliana*) "omics" data. All three *F. pringlei* CAs have orthologs in the closely related C<sub>4</sub> plant *Flaveria bidentis*, and comparisons of ortholog sequences, expression patterns, and intracellular locations of their products indicated that CA1 and CA2 have maintained their ancestral role in C<sub>4</sub> plants, whereas modifications to the C<sub>3</sub> CA3 gene led to the evolution of the CA isoform that catalyzes the first step in the C<sub>4</sub> photosynthetic pathway. These changes included the loss of the chloroplast transit peptide and an increase in gene expression, which resulted in the high levels of CA activity seen in the cytosol of C<sub>4</sub> mesophyll cells.

At least 45 independent origins of the C<sub>4</sub> photosynthetic pathway from the ancestral C<sub>3</sub> pathway have occurred within the angiosperms (Sage, 2004). The primary driver for the evolution of the pathway is believed to be the reduction in atmospheric CO<sub>2</sub> concentrations to near present-day levels, which were reached at the Oligocene/Miocene boundary about 24 million years ago, with other environmental factors

such as heat, aridity, and salinity also playing important roles in the development and expansion of the C<sub>4</sub> syndrome (Sage, 2004; Osborne and Beerling, 2006; Tipple and Pagani, 2007; Christin et al., 2008; Vicentini et al., 2008). The plants that evolved as a result of these selective pressures were able to concentrate CO<sub>2</sub> in their leaves because of an exquisite blend of anatomy and biochemistry (Hatch, 1987). In contrast, in this reduced atmospheric CO<sub>2</sub> world, C<sub>3</sub> plants showed losses in assimilated CO<sub>2</sub> and increased photorespiratory rates due to increased oxygenase activity of Rubisco. These responses were only exacerbated in hot, dry, high-light, and saline conditions, and consequently, C<sub>3</sub> plants were out-competed by C<sub>4</sub> species in such environments (Ehleringer and Monson, 1993; Long, 1999).

Unlike C<sub>3</sub> plants, in which all of the reactions of photosynthesis take place in leaf mesophyll cells, in most terrestrial C<sub>4</sub> plants, two cell types, the mesophyll cells and bundle sheath cells, are involved in the reactions of CO<sub>2</sub> assimilation. In C<sub>4</sub> leaves, the acquisition of atmospheric CO<sub>2</sub> occurs in the cytosol of mesophyll cells when the enzyme carbonic anhydrase (CA) converts CO<sub>2</sub> to bicarbonate, which is then used by the primary carboxylase of C<sub>4</sub> plants, phosphoenolpyruvate carboxylase (PEPC; Hatch and Burnell, 1990), to form a C<sub>4</sub> acid. The four-carbon acid diffuses

<sup>1</sup> This work was supported by the Australian Research Council. S.K.T. was the recipient of an International Macquarie University Research Scholarship.

<sup>2</sup> Present address: ARC Centre of Excellence in Plant Energy Biology, University of Western Australia, 35 Stirling Highway, Crawley, Western Australia 6009, Australia.

<sup>3</sup> Present address: Department of Chemistry and Biomolecular Sciences, Macquarie University, Sydney, New South Wales 2109, Australia.

\* Corresponding author; e-mail mludwig@cyllene.uwa.edu.au.

The author responsible for distribution of materials integral to the findings presented in this article in accordance with the policy described in the Instructions for Authors ([www.plantphysiol.org](http://www.plantphysiol.org)) is: Martha Ludwig (mludwig@cyllene.uwa.edu.au).

[C] Some figures in this article are displayed in color online but in black and white in the print edition.

[OA] Open Access articles can be viewed online without a subscription.

[www.plantphysiol.org/cgi/doi/10.1104/pp.109.137513](http://www.plantphysiol.org/cgi/doi/10.1104/pp.109.137513)

into a neighboring bundle sheath cell, where it is decarboxylated. Rubisco and the other enzymes of the photosynthetic carbon reduction cycle, located in the bundle sheath cell chloroplasts, reduce the released CO<sub>2</sub> and the remaining three-carbon compound diffuses back into the mesophyll cells, where it can undergo another round of the C<sub>4</sub> acid cycle. This combination of anatomical and biochemical characteristics, including the cell-specific expression of enzymes, results in an efficient CO<sub>2</sub> concentrating mechanism whereby the CO<sub>2</sub> level in the C<sub>4</sub> bundle sheath cells is up to 20 times that of the surrounding mesophyll cells and photorespiration is essentially eliminated (Jenkins et al., 1989).

The enzymes catalyzing the steps in the C<sub>4</sub> pathway are also present in C<sub>3</sub> plants, and several, including PEPC (Hermans and Westhoff, 1990; Kawamura et al., 1992; Gowik et al., 2006), NADP-malic enzyme (Rajeevan et al., 1991; Marshall et al., 1996; Drincovich et al., 1998; Lai et al., 2002; Tausta et al., 2002), and pyruvate orthophosphate dikinase (Rosche et al., 1994; Imaizumi et al., 1997), have been examined in the context of C<sub>4</sub> evolution. Many of these studies (Hermans and Westhoff, 1990; Rajeevan et al., 1991; Rosche et al., 1994; Marshall et al., 1996; Drincovich et al., 1998; Lai et al., 2002) used members of the genus *Flaveria* as model organisms for understanding the steps involved in the evolution of C<sub>4</sub> photosynthesis, because this group of closely related plants contains individual species demonstrating C<sub>3</sub>, C<sub>4</sub>, or intermediate C<sub>3</sub>-C<sub>4</sub> photosynthesis, indicating that the evolution toward C<sub>4</sub> photosynthesis is ongoing in this genus (McKown et al., 2005). The results from several of these studies demonstrated that the genes encoding the enzymes important in C<sub>4</sub> photosynthesis evolved through the duplication of ancestral C<sub>3</sub> genes followed by the neofunctionalization of one copy, which involved increased gene expression in specific organs and cell types (for review, see Monson, 2003). The other copies of the duplicated genes, which encode the C<sub>3</sub> forms of the enzymes and are involved in housekeeping functions, were maintained in the C<sub>4</sub> species and show levels of expression similar to those exhibited in C<sub>3</sub> species.

We are studying the enzyme CA (EC 4.2.1.1) in *Flaveria* species, which demonstrate different photosynthetic pathways, to gain insights into the evolution of C<sub>4</sub> photosynthesis (Ludwig and Burnell, 1995; Tetu et al., 2007). We have shown that a small multigene family encodes  $\beta$ -CA in the C<sub>4</sub> species *Flaveria bidentis* and that the expression patterns of three of its members are organ specific. One of the genes, CA3, encodes the cytosolic form of the enzyme that is highly expressed in leaves and is responsible for catalyzing the first step in the C<sub>4</sub> pathway, providing PEPC with bicarbonate in mesophyll cells (von Caemmerer et al., 2004; Tetu et al., 2007). *F. bidentis* CA2 is also a cytosolic enzyme; however, its cognate gene is expressed at similar levels in both photosynthetic and nonphotosynthetic tissues and the enzyme probably supplies

bicarbonate to nonphotosynthetic forms of PEPC for anaplerotic functions (Tetu et al., 2007). *F. bidentis* also contains a chloroplastic  $\beta$ -CA, CA1, which is likely to be encoded by an ortholog of the ancestral C<sub>3</sub> gene whose protein product is the CA that is active in C<sub>3</sub> mesophyll chloroplasts (Poincelot, 1972; Jacobson et al., 1975; Tsuzuki et al., 1985), and may make up to 2% of soluble leaf protein in C<sub>3</sub> species (Okabe et al., 1984; Cowan, 1986).

Although CA is an abundant and active protein in C<sub>3</sub> plants, the number of CA isoforms encoded by a C<sub>3</sub> species and their intracellular locations have been determined only for *Arabidopsis* (*Arabidopsis thaliana*; Fabre et al., 2007). Furthermore, no unequivocal role has yet been assigned to any C<sub>3</sub> plant CA isoform. It has been suggested that C<sub>3</sub> chloroplastic  $\beta$ -CAs are responsible for maintaining adequate levels of CO<sub>2</sub> for Rubisco by facilitating the diffusion of CO<sub>2</sub> across the chloroplast envelope or through the rapid dehydration of bicarbonate to CO<sub>2</sub> (Reed and Graham, 1981; Cowan, 1986; Price et al., 1994). However, CA antisense and gene knockout studies have shown no significant impairment in CO<sub>2</sub> assimilation in mature plant leaves (Majeau et al., 1994; Price et al., 1994; Williams et al., 1996; Ferreira et al., 2008). Other work has suggested that chloroplastic  $\beta$ -CAs may have nonphotosynthetic roles, appearing to be involved in lipid biosynthesis (Hoang and Chapman, 2002) and disease resistance (Slaymaker et al., 2002; Restrepo et al., 2005; Wang et al., 2009) in C<sub>3</sub> plants. Interestingly, levels of a chloroplastic  $\beta$ -CA and a cytosolic  $\beta$ -CA increased during greening of *Arabidopsis* seedlings, and while levels of transcripts encoding the cytosolic enzyme mirrored those of the protein, transcript abundance for the chloroplastic enzyme did not change (Wang et al., 2006). Cytosolic  $\beta$ -CAs of C<sub>3</sub> plants have been implicated in the provision of bicarbonate for nonphotosynthetic forms of PEPC (Fett and Coleman, 1994; Raven and Newman, 1994; Chollet et al., 1996).

Here, we show that  $\beta$ -CA orthologs of *F. bidentis* CA1, CA2, and CA3 are present in the C<sub>3</sub> species *Flaveria pringlei* and that each CA gene exhibits organ-specific expression patterns in this C<sub>3</sub> plant. We also report the intracellular location of the three CA isoforms, consider their probable physiological functions, and discuss these data in the context of the evolution of the C<sub>4</sub> photosynthetic pathway.

## RESULTS

### *F. pringlei* $\beta$ -CA cDNAs

Western- and northern-blot analyses of a previous study suggested that a small multigene family codes for  $\beta$ -CA in *F. pringlei* (Ludwig and Burnell, 1995); however, only a single cDNA encoding the enzyme designated CA1 was isolated and described (GenBank accession no. U19737). cDNAs encoding two additional, distinct  $\beta$ -CA isoforms in *F. pringlei* leaf tissue,

named CA2 and CA3, were obtained in the present study using a RACE PCR approach with a *F. pringlei* leaf adaptor-ligated cDNA library and primers based on CA sequences from the closely related *F. bidentis* (GenBank accession nos. AY167112 and AY167113).

The *F. pringlei* CA2 cDNA isolated was 1,178 bp and encoded an open reading frame (ORF) of 843 bp, which was predicted to code for a polypeptide of 281 amino acids with a molecular mass of 30.7 kD. Two in-frame, upstream stop codons at positions -6 and -84, relative to the proposed translation start site, were encoded in the 87-bp 5' noncoding sequence, while the 245-bp 3' noncoding sequence contained two putative polyadenylation signals, AATAAC and AATAAT (Dean et al., 1986), located 44 and 159 nucleotides from the proposed termination codon, respectively.

A 984-bp ORF was encoded by the *F. pringlei* CA3 cDNA, along with 32 and 141 bp of 5' and 3' noncoding sequence, respectively. An in-frame stop codon was found at position -6 relative to the proposed initiating Met, and a putative polyadenylation signal, AATAAA (Dean et al., 1986), was found at position 1,080 of the cDNA. The ORF was predicted to encode a polypeptide of 328 amino acids with a molecular mass of 35.2 kD.

All of the amino acids corresponding to the pea (*Pisum sativum*)  $\beta$ -CA active site residues, namely Gln-151, Asp-162, Arg-164, Phe-179, Val-184, Tyr-205, and Gly-224 (Kimber and Pai, 2000), are found in analogous positions in the *F. pringlei* CAs, except that Val-184 is replaced with an Ile residue in CA2, as is the case for *F. bidentis* CA2 (Fig. 1; Tetu et al., 2007). One His and two Cys residues, corresponding to His-220, Cys-160, and Cys-223 in the pea CA sequence and thought to coordinate the catalytic zinc ion (Provart et al., 1993; Bracey et al., 1994; Kimber and Pai, 2000), are also present in all of the *F. pringlei* CA sequences (Fig. 1).

A comparison of the predicted amino acid sequences of the three *F. pringlei* CAs showed that CA2 shares 51% and 53% identity with CA1 and CA3, respectively, while the CA3 and CA1 polypeptides are 73% identical (Table I; Fig. 1). The deduced amino acid sequence of *F. pringlei* CA1 is 97% identical to that of the CA1 isoform from the C<sub>4</sub> species *F. bidentis* (Table I; Fig. 1; Ludwig and Burnell, 1995). A high level of sequence identity (93%) is also seen between *F. pringlei* and *F. bidentis* CA2 isoforms, while the CA3 proteins from the two species are 73% identical (Table I; Fig. 1). Higher sequence identity is seen between the two CA3 isoforms when they are compared over their shared region; the two sequences are 93% identical when the first 71 residues are excluded from the *F. pringlei* CA3 sequence.

Pairwise comparisons of the predicted *F. pringlei* CA amino acid sequences with those of the six  $\beta$ -CA isoforms identified in Arabidopsis (Fabre et al., 2007) showed that *F. pringlei* CA1 and CA3 share 66% sequence identity with At $\beta$ CA1 from Arabidopsis, while *F. pringlei* CA2 shows the highest identity to At $\beta$ CA4 (Table I). These relationships were supported

in a phylogenetic tree constructed using the neighbor-joining method (Saitou and Nei, 1987) and the predicted  $\beta$ -CA amino acid sequences from *F. pringlei*, *F. bidentis*, and five other dicots (*Arabidopsis*, *Glycine max*, *Medicago truncatula*, *Populus trichocarpa*, and *Vitis vinifera*), three monocots (*Oryza sativa japonica*, *Sorghum bicolor*, and *Zea mays*), a lycopod (*Selaginella moellendorffii*), and a moss (*Physcomitrella patens*) for which whole genome sequence information is known (Fig. 2). Midpoint rooting of this tree resolved the CA sequences into two major clusters, clades A and B. Clade A consists only of angiosperm CA sequences, with a dicot clade in which all of the *Flaveria* CA sequences cluster and a smaller monocot clade. Clade B contains the CA sequences from the primitive plants in addition to angiosperm CA sequences. The clustering of *F. pringlei* CA1 and CA3 sequences with those of *F. bidentis* indicates that these isoforms share a common ancestry and have resulted from a duplication event of the gene encoding CA1 after the divergence of *Flaveria* from the other dicots represented in this part of the tree, but before *F. pringlei* and *F. bidentis* diverged from one another. The two Arabidopsis CA sequences, At $\beta$ CA1 and At $\beta$ CA2, which show the greatest sequence identity of all the Arabidopsis CAs to *F. pringlei* CA1 and CA3 (Table I), are in the sister clade and are a result of a large segmental duplication of the Arabidopsis genome (Arabidopsis Genome Initiative, 2000). The CA2 sequences from *F. pringlei* and *F. bidentis* also cluster tightly; however, they are in a clade distinct from that containing the CA1 and CA3 sequences. Two Arabidopsis sequences, At $\beta$ CA3 and At $\beta$ CA4, which have also arisen through the duplication of a large segment of the Arabidopsis genome (Arabidopsis Genome Initiative, 2000), cluster with the *Flaveria* CA2 sequences, along with sequences encoding CA isoforms from two legumes and a woody plant.

To examine the complexity of the *F. pringlei*  $\beta$ -CA multigene family, genomic Southern-blot analyses were done. Total genomic DNA from *F. pringlei* leaf tissue, digested with restriction enzymes that did not cut within the CA1, CA2, or CA3 ORFs, was probed with a <sup>32</sup>P-radiolabeled 633-bp fragment liberated from the *F. pringlei* CA2 cDNA by HindIII digestion (Fig. 3). As *F. pringlei* CA1 and CA3 cDNAs share 66% sequence identity with CA2 over the region encoded by the probe, it was expected that the probe would hybridize to fragments encoding these CA genes as well as any additional closely related sequences. EcoRI digestion of *F. pringlei* genomic DNA produced two intensely labeled fragments of approximately 3.5 and 1.7 kb as well as three weakly hybridized bands of 7.6, 2.8, and 0.56 kb (Fig. 3). A relatively simple labeling pattern was also seen in XbaI digests of *F. pringlei* genomic DNA. Three fragments of approximately 8, 2.4, and 2.2 kb were strongly labeled, with two weakly hybridized bands of 1.7 and 1.6 kb also detected (Fig. 3). These results confirm that  $\beta$ -CA is encoded by a small multigene family in *F. pringlei* (Ludwig and Burnell, 1995).

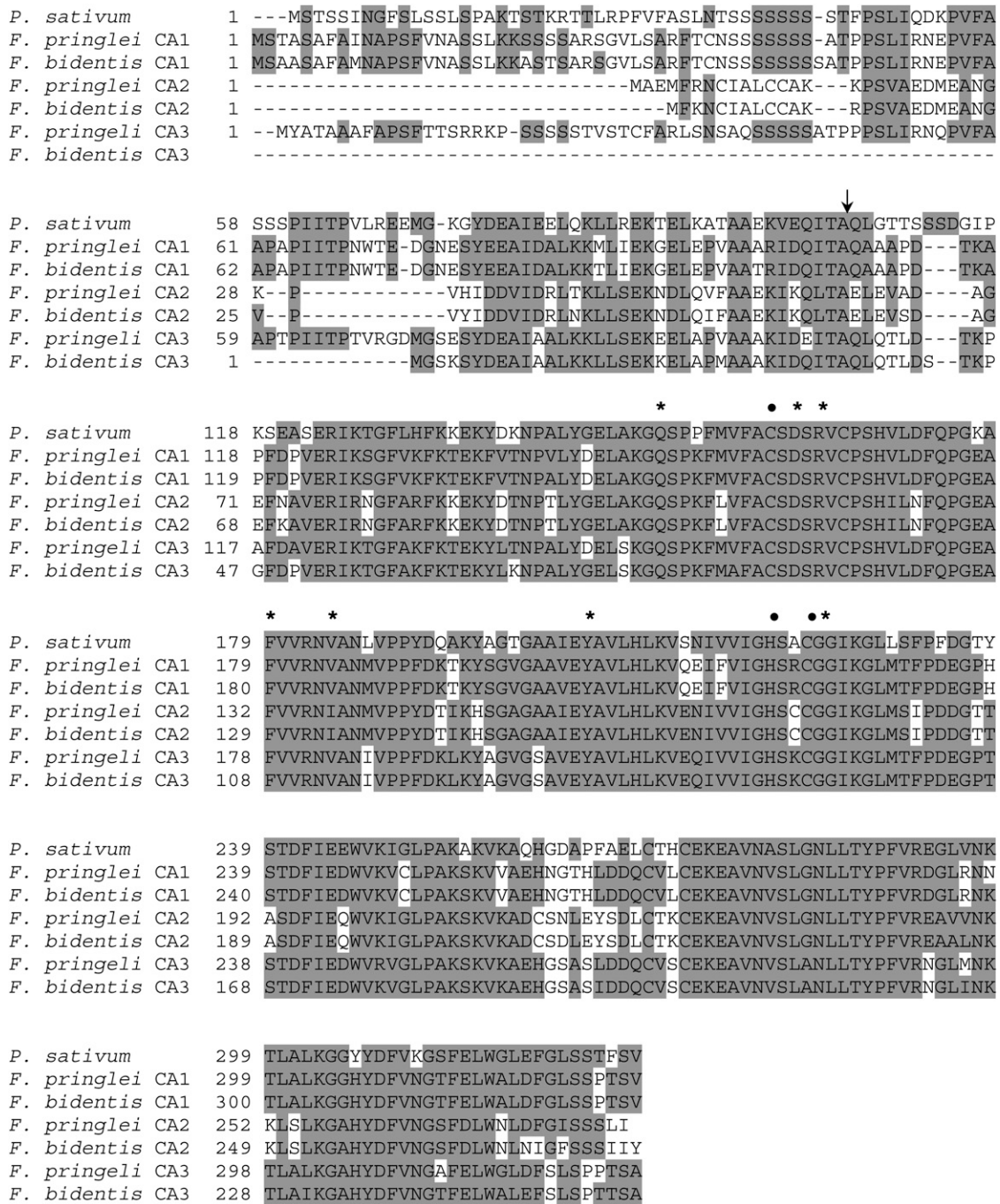


**Figure 1.** Alignment of the deduced amino acid sequences of *F. pringlei*  $\beta$ -CAs with those of *F. bidentis* and pea. Identical amino acids and conservative changes are shaded. Dashes represent gaps inserted to maximize the alignment. Amino acids in the proposed active site and those acting as zinc ligands, based on the pea  $\beta$ -CA sequence (Kimber and Pai, 2000), are marked with asterisks and dots, respectively. The arrow denotes the predicted cleavage site in plastidial C<sub>3</sub> dicot  $\beta$ -CAs (Burnell et al., 1990; Roeske and Ogren, 1990). GenBank accession numbers are as follows: pea, M63627; *F. bidentis* CA1, U08398; *F. bidentis* CA2, AY167112; *F. bidentis* CA3, AY167113.

**$\beta$ -CA Gene Expression in *F. pringlei* Organs**

To elucidate the locations and the possible physiological roles of the three *F. pringlei*  $\beta$ -CA isoforms, the expression patterns of their cognate genes in photo-

synthetic and nonphotosynthetic tissues were determined using quantitative reverse transcription (qRT)-PCR. Overall CA gene transcript levels were at least 2 orders of magnitude higher in *F. pringlei* leaves than in

**Table 1.** Identity matrix of *F. pringlei*, *F. bidentis*, and *Arabidopsis*  $\beta$ -CA predicted amino acid sequences

Pairwise alignments were made using ClustalW, and percentage identities were determined using MacVector 9.0 Sequence Analysis Software (Accelrys). FpCA1 to FpCA3, *F. pringlei* CA1 to CA3; FbCA1 to FbCA3, *F. bidentis* CA1 to CA3 (Tetu et al., 2007); At $\beta$ CA1 to At $\beta$ CA6, *Arabidopsis*  $\beta$ -CA1 to  $\beta$ -CA6 (Fabre et al., 2007).

	FpCA1	FpCA2	FpCA3	FbCA1	FbCA2	FbCA3	At $\beta$ CA1	At $\beta$ CA2	At $\beta$ CA3	At $\beta$ CA4	At $\beta$ CA5	At $\beta$ CA6
FpCA1	100%											
FpCA2	51%	100%										
FpCA3	73%	53%	100%									
FbCA1	97%	51%	73%	100%								
FbCA2	50%	93%	52%	50%	100%							
FbCA3	61%	59%	73%	61%	59%	100%						
At $\beta$ CA1	66%	49%	66%	66%	49%	56%	100%					
At $\beta$ CA2	55%	59%	55%	55%	58%	69%	65%	100%				
At $\beta$ CA3	43%	56%	44%	43%	56%	56%	42%	56%	100%			
At $\beta$ CA4	48%	61%	50%	47%	60%	57%	45%	54%	69%	100%		
At $\beta$ CA5	32%	36%	32%	32%	34%	32%	31%	33%	35%	37%	100%	
At $\beta$ CA6	24%	29%	27%	24%	29%	32%	23%	30%	30%	31%	38%	100%

root and flower tissues (Fig. 4), with transcripts from all three CA genes detected in leaves (Fig. 4A). In contrast to this, in roots and flowers, only CA1 and CA2 mRNAs were measurable (Fig. 4, B and C); however, both were much lower in abundance in nongreen tissues than in leaves.

The relative abundance of CA gene-specific transcripts also differed between the organs. In the leaves of the three *F. pringlei* plants tested, CA1 and CA3 mRNA levels were essentially equal and at least 10 times higher than those of CA2 transcripts (Fig. 4A). In contrast, steady-state levels of CA2 gene transcripts were at least 150 times more abundant than CA1 mRNA levels in the root tissues of the three plants examined, while CA3 mRNA was not detected in these tissues (Fig. 4B). The CA2 gene was also the most highly expressed of the three CA genes in *F. pringlei* flowers. CA2 mRNA levels were at least 12 times higher than CA1 transcripts and, as in roots, CA3 gene activity was not detected in flowers.

#### Localization of *F. pringlei* $\beta$ -CA Isoforms

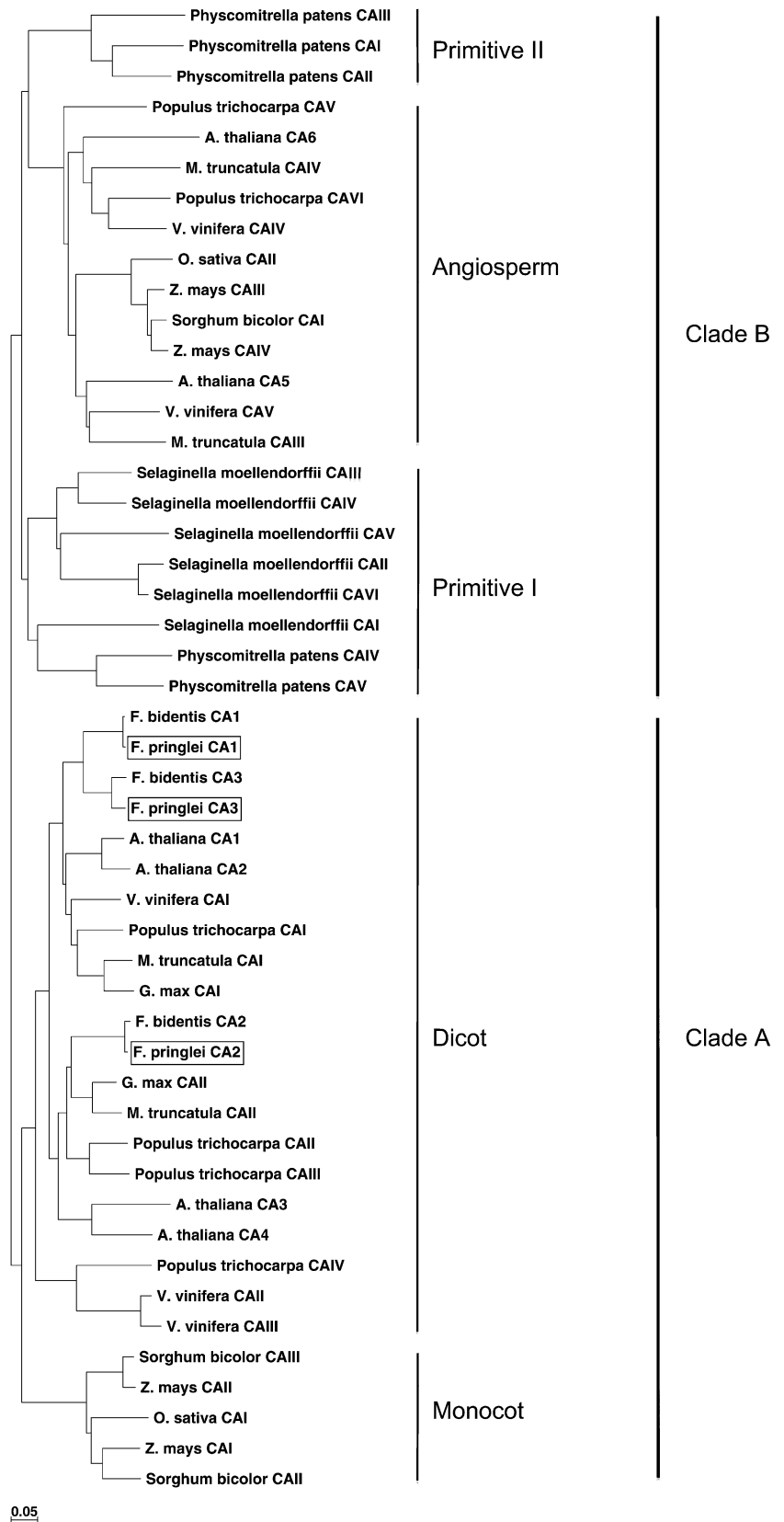
An affinity-purified, anti-*F. bidentis* CA3 antiserum (Tetu et al., 2007) was used to immunolocalize  $\beta$ -CAs in *F. pringlei* leaves. Three polypeptides of approximately 32 kD and a doublet of 28 and 30 kD were intensely labeled on immunoblots of *F. pringlei* leaf extracts following SDS-PAGE (Fig. 5A). When transverse sections of *F. pringlei* leaves were labeled for immunofluorescence microscopy with the same antiserum, fluorescence was detected at the periphery of the cells, in the thin layer of cytoplasm surrounding the large central vacuole (Fig. 5D). Comparison of immunolabeled sections with methylene blue-stained transverse sections (Fig. 5, B and C) showed that most of the labeling was composed of rings of bright fluorescent dots surrounding the large starch grains, which filled most of the mesophyll chloroplasts (Fig. 5, compare C and D). A lower level of fluorescence was

detected in the cytoplasm (Fig. 5D). Only background autofluorescence was detected in *F. pringlei* leaf sections labeled with preimmune serum in place of the anti-*F. bidentis* CA3 antibody (Fig. 5E).

Sequence comparisons (Fig. 1) indicated that the N-terminal regions of *F. pringlei* CA1 and CA3 exhibit characteristics of chloroplast transit peptides, having a low number of charged amino acids but being relatively enriched in hydroxylated residues (von Heijne et al., 1989). In contrast, the N-terminal region of *F. pringlei* CA2 does not demonstrate these properties (Fig. 1). The cleavage site for the transit peptide of chloroplast-targeted  $\beta$ -CAs has been determined empirically for spinach (*Spinacia oleracea*; Burnell et al., 1990) and pea (Roeske and Ogren, 1990) by N-terminal sequencing of the purified enzymes, with the mature proteins starting at Gln-106 and Glu-98, respectively. Interestingly, the amino acid residues immediately N terminal to these processing sites are highly conserved among plant  $\beta$ -CAs (Fig. 1), regardless of whether the N terminus appears to encode a chloroplast transit peptide. In silico analyses using protein targeting prediction programs, including ChloroP (Emanuelsson et al., 1999), TargetP (Emanuelsson et al., 2000), Predotar (Small et al., 2004), iPSORT (Bannai et al., 2002), and WoLF PSORT (Horton et al., 2007), also consistently predicted the presence of a transit peptide and/or a location in the chloroplast for *F. pringlei* CA1 and CA3, whereas no clear location or a cytosolic location was predicted for *F. pringlei* CA2 (data not shown).

Since sequence analysis and protein targeting prediction programs provide only an indication of the intracellular location of a protein, in vitro chloroplast import studies were done to determine which of the *F. pringlei*  $\beta$ -CA isoforms localize to the organelle. When in vitro transcribed and translated *F. pringlei* CA1 and CA3 precursor proteins (Fig. 6, lane 1) were incubated with pea chloroplasts under conditions that supported import, lower molecular mass forms of the proteins were detected in the chloroplast pellets (Fig. 6, lane 2).

**Figure 2.** Midpoint rooted neighbor-joining tree of selected plant  $\beta$ -CA sequences. Two major clades, clades A and B, are resolved from predicted  $\beta$ -CA amino acid sequences of selected monocots, dicots, a moss, and a lycopod (see "Materials and Methods" for details). *F. pringlei* CAs are boxed. The bar represents 5% sequence divergence.



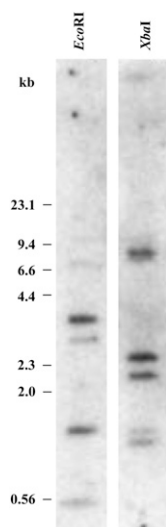


**Figure 3.** Genomic Southern-blot analysis of *F. pringlei*  $\beta$ -CA genes. Genomic DNA (10  $\mu$ g) isolated from *F. pringlei* leaf tissue was digested to completion with *Eco*RI and *Xba*I. DNA fragments were separated on a 0.8% agarose gel, blotted to a positively charged nylon membrane, and hybridized with a <sup>32</sup>P-labeled 633-bp *Hind*III restriction fragment derived from *F. pringlei* CA2. Molecular size markers in kb are indicated.

This was also the case for the small subunit (SSU) of Rubisco, which served as a positive import control protein (Fig. 6, lanes 1 and 2). These processed proteins were protected from digestion by the protease thermolysin due to their location within the chloroplasts (Fig. 6, lane 3). In contrast, *F. pringlei* CA2 does not localize to the chloroplast. Import assays involving CA2 precursor protein (Fig. 6, lane 1) did not result in the appearance of a lower molecular mass polypeptide in the chloroplast fraction (Fig. 6, lane 2), nor could the precursor protein be detected after thermolysin was added to the assays (Fig. 6, lane 3). No clear correspondence was seen between the sizes of the precursor and/or imported CA isoforms and the immunoreactive polypeptides in *F. pringlei* whole leaf extracts. This is probably largely due to differences between post-translational modifying mechanisms of *F. pringlei* chloroplasts and the heterologous *in vitro* system.

## DISCUSSION

We are focused on understanding the steps involved in the molecular evolution of the C<sub>4</sub> photosynthetic pathway from the more ancestral C<sub>3</sub> pathway. We have concentrated our attention on the evolution of  $\beta$ -CA isoforms that are involved in both CO<sub>2</sub> assimilation pathways, and we have used the genus *Flaveria* as a model system for our studies because it contains individual species that demonstrate C<sub>3</sub>, C<sub>4</sub>, or C<sub>3</sub>-C<sub>4</sub> intermediate photosynthesis (Ludwig and Burnell, 1995; Tetu et al., 2007). We have recently characterized

the  $\beta$ -CA isoforms prevalent in the leaf tissue of the C<sub>4</sub> species *F. bidentis* with respect to their gene expression patterns and intracellular locations (Tetu et al., 2007). Here, we have shown that, as in *F. bidentis*, *F. pringlei*  $\beta$ -CAs are encoded by a small multigene family, that *F. pringlei*  $\beta$ -CA genes also exhibit organ-specific expression, and that there are cytosolic and chloroplastic forms of the enzyme in this C<sub>3</sub> species. These studies have not only identified the dominant  $\beta$ -CA isoforms

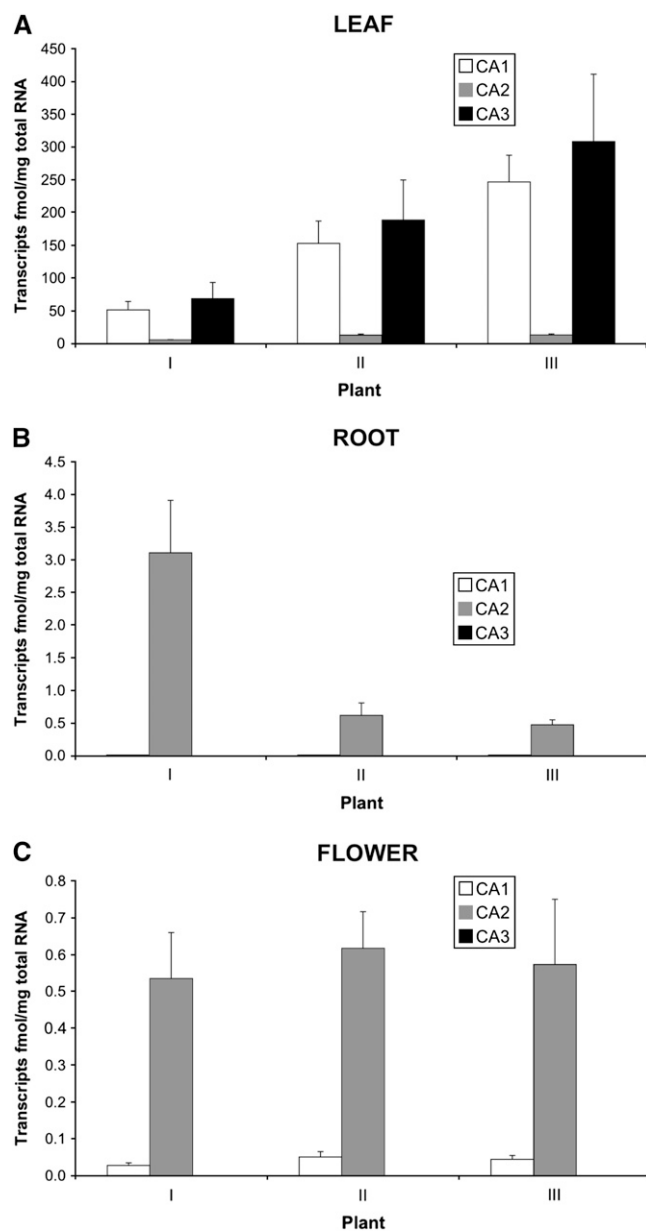


**Figure 4.**  $\beta$ -CA gene transcript abundance in *F. pringlei* organs. Total RNA was isolated from leaves (A), roots (B), and flowers (C) of three individual *F. pringlei* plants (I, II, and III), and  $\beta$ -CA transcript abundance was measured using qRT-PCR. Results are expressed on a total RNA basis. Error bars represent the SE of at least three independent reactions.



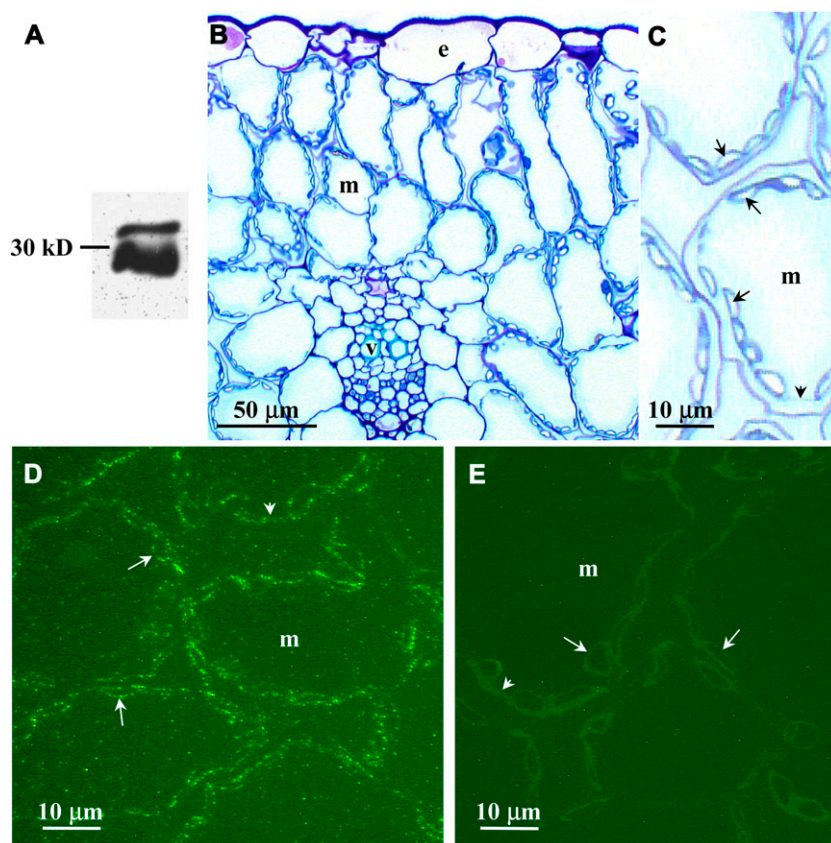


**Figure 5.** Immunolocalization of *F. pringlei*  $\beta$ -CA. A, *F. pringlei* soluble leaf proteins were separated by SDS-PAGE, blotted to nitrocellulose, and labeled with an affinity-purified anti-*F. bidentis* CA3 antiserum. Immunoreactive polypeptides of approximately 32 kD and a doublet of 30 and 28 kD were detected using a horseradish peroxidase-conjugated secondary antibody and an enhanced chemiluminescence method. B, A transverse section through a fixed and embedded *F. pringlei* leaf stained with methylene blue shows characteristic  $C_3$  leaf anatomy, with most of the interior of the leaf composed of mesophyll cells (m). C, A section through several mesophyll cells stained with methylene blue at higher magnification shows numerous chloroplasts containing starch grains (arrows) in the peripheral cytoplasm (arrowhead) of the cells. D, A transverse leaf section immunolabeled with an affinity-purified anti-*F. bidentis* CA3 antiserum followed by an AlexaFluor 488-conjugated secondary antibody. Labeling in the chloroplasts of mesophyll cells appears as rings of bright fluorescent dots surrounding the starch grains (arrows). Less intense labeling is seen in the cytoplasm (arrowhead). E, A transverse section labeled with preimmune serum followed by the AlexaFluor 488-conjugated secondary antibody. No fluorescence is detected in the mesophyll cell chloroplasts (arrows), cytoplasm (arrowhead), or elsewhere in the cells. e, Epidermal cell; v, vascular bundle. [See online article for color version of this figure.]

in the leaves of these species but also offer the unique opportunity to compare the structure, expression patterns, and putative functions of leaf  $\beta$ -CAs from two closely related species that use different photosynthetic pathways, thereby allowing the identification of molecular changes that occurred in  $\beta$ -CA genes during the evolution of  $C_4$  photosynthesis.

#### *F. pringlei* Leaf $\beta$ -CA Isoforms Show High Homology to Other Plant $\beta$ -CAs

Three cDNAs encoding distinct  $\beta$ -CA isoforms were isolated from *F. pringlei* leaf  $\lambda$ gt11D (CA1; Ludwig and Burnell, 1995) and adaptor-ligated (CA2 and CA3; this study) cDNA libraries. Our genomic Southern-blot analyses are consistent with the *F. pringlei* genome

encoding three  $\beta$ -CA genes; however, we cannot exclude the existence of other members of this multigene family. If additional  $\beta$ -CA genes are present in *F. pringlei*, then their expression levels are very low and/or their transcripts are highly unstable, as multiple screens of all our *F. pringlei* cDNA libraries, as well as numerous RT-PCR assays using cDNA derived from various organs and multiple plants, have not yielded fragments encoding other distinct  $\beta$ -CA isoforms. As shown in Figure 2, current information from whole genome sequencing projects indicates that between two and six distinct CA isoforms are encoded in the genomes of terrestrial plants. Whether a correlation exists between the taxonomic position of a species and the number of  $\beta$ -CAs its genome encodes awaits further whole genome sequence determination.



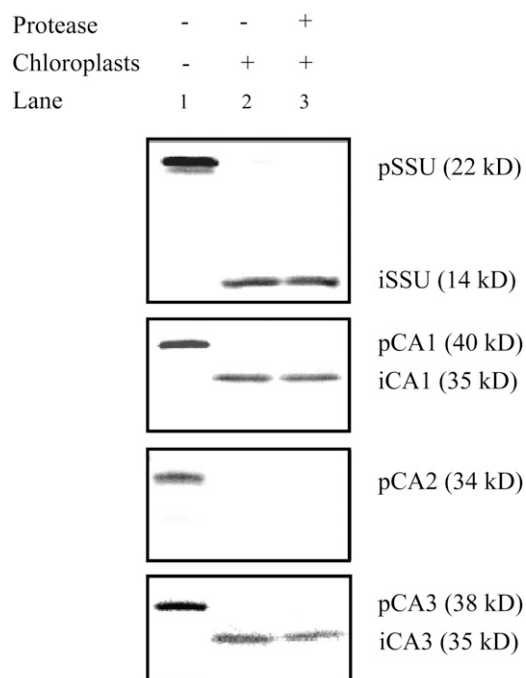


**Figure 6.** In vitro chloroplast import analysis of *F. pringlei*  $\beta$ -CA precursor proteins. Precursor proteins of pea Rubisco SSU (pSSU) and *F. pringlei* CA1 (pCA1), CA2 (pCA2), and CA3 (pCA3) were synthesized using [<sup>35</sup>S]Met and a coupled transcription/translation rabbit reticulocyte lysate system and then used in import assays with isolated pea chloroplasts. Lane 1, Precursor proteins; lane 2, chloroplast fraction following incubation with the precursor proteins under conditions favoring import; lane 3, as for lane 2 but with the addition of thermolysin following the import assay. Molecular masses of the precursor and imported (i) proteins are indicated on the right.

The amino acid sequences deduced from the *F. pringlei* CA cDNAs showed identity to the predicted  $\beta$ -CA sequences from other C<sub>3</sub> and C<sub>4</sub> plants. Residues required for the formation of the active site cleft (Kimber and Pai, 2000) and coordination of the zinc ion in the active site of pea  $\beta$ -CA (Provart et al., 1993; Bracey et al., 1994; Kimber and Pai, 2000) were in equivalent positions in all of the *F. pringlei* CA sequences with one exception. *F. pringlei* CA2 has an Ile at the position corresponding to Val-184 of pea  $\beta$ -CA. In pea  $\beta$ -CA, this residue is thought to contribute to a continuous hydrophobic surface in the binding pocket (Kimber and Pai, 2000). As the side chain of Ile is more nonpolar than that of Val, the hydrophobic nature of the pocket would be maintained with the former residue. The CA2 orthologs from *F. bidentis* (Fig. 1; Tetu et al., 2007), the C<sub>3</sub>-C<sub>4</sub> intermediate species, *Flaveria linearis* (GenBank accession no. U19740), and all of the Arabidopsis  $\beta$ -CA isoforms except At $\beta$ CA6 (Fabre et al., 2007) also have an Ile in this position.

Reconstruction of the phylogenetic relationships between  $\beta$ -CA sequences from two primitive plants and angiosperms, including monocots and herbaceous and woody dicots, showed the sequences clustered

into two large clades. One clade contained the sequences of some angiosperm  $\beta$ -CAs and all those of the primitive plants. In contrast, the other major clade contained  $\beta$ -CA sequences from only angiosperms, and all of the *Flaveria* sequences used in the analysis clustered in two sister groups within it. The positions of the *Flaveria* CA1 and CA3 sequences in the phylogeny indicate that they have arisen through a duplication of the gene encoding a chloroplastic form of the enzyme in the ancestral C<sub>3</sub> *Flaveria* species. Mutations in coding and control regions of the CA3 gene in the C<sub>4</sub> species then resulted in the changes in intracellular location and expression demonstrated by the present-day C<sub>4</sub> enzyme (see below).

Although localization information is known for all of the  $\beta$ -CA isoforms in just three species represented in our neighbor-joining tree, *Arabidopsis*, *F. pringlei*, and *F. bidentis*, it is worthwhile noting that there is no consistent correlation between the phylogenetic position of a  $\beta$ -CA isoform and its intracellular location. For example, chloroplastic CAs from *F. pringlei* (CA1 and CA3) and chloroplastic (At $\beta$ CA1) and cytosolic (At $\beta$ CA2) CAs from *Arabidopsis* (Fabre et al., 2007) share relatively high sequence identity and cluster together in the tree. The At $\beta$ CA1 and At $\beta$ CA2 genes, as well as those encoding At $\beta$ CA3 and At $\beta$ CA4, which localize to the cytosol and plasma membrane, respectively (Fabre et al., 2007) and also cluster tightly in the tree, evolved from large segmental duplications of the *Arabidopsis* genome with subsequent divergence (*Arabidopsis* Genome Initiative, 2000). As for *F. pringlei* CA1 and CA3, the evolutionary relationships of the *Arabidopsis* genes and the intracellular locations of the encoded proteins strongly support the notion that gene duplication events provide the material for genome evolution, including the potential for novel gene pathways and differential gene expression patterns (Zhang, 2003).

#### *F. pringlei* Contains Two Chloroplastic $\beta$ -CAs

Most CA activity in C<sub>3</sub> species is found in the stroma of mesophyll cell chloroplasts (Poincelot, 1972; Jacobson et al., 1975; Tsuzuki et al., 1985), and recent work on the oligomeric stromal proteome of *Arabidopsis* showed that At $\beta$ CA1 is a prevalent protein in this subcellular compartment, making up about 1% of the total stromal mass (Peltier et al., 2006).

Our results also indicate that  $\beta$ -CAs are abundant proteins in the photosynthetic tissues of *F. pringlei*. Transcripts from all three CA genes were detected in the first fully expanded leaves of *F. pringlei* plants using qRT-PCR. CA1 and CA3 gene transcripts were of equal abundance in the three plants tested and 1 order of magnitude greater than steady-state levels of CA2 mRNA. Although there is not always a direct correlation between transcript abundance and protein amount (Gygi et al., 1999), our immunoblot analyses showed that  $\beta$ -CA is a prevalent protein in *F. pringlei* leaves; three polypeptides in leaf protein extracts of

approximately 32 kD and a doublet of 30 and 28 kD labeled strongly with an antiserum generated against *F. bidentis* CA3. The relative mobilities of these polypeptides agree with the sizes predicted from their deduced amino acid sequences when the putative cleavage site of chloroplastic  $\beta$ -CAs (Fig. 1; Burnell et al., 1990; Roeske and Ogren, 1990) is used for CA1 and CA3. The doublet in Figure 5A represents the two chloroplastic isoforms, while the largest immunoreactive protein corresponds to the cytosolic CA2, which is unprocessed. We previously reported the detection of two immunoreactive proteins using an anti-spinach  $\beta$ -CA antiserum to probe *F. pringlei* leaf protein extracts (Ludwig and Burnell, 1995); however, upon closer inspection, the lower labeled band on these earlier blots has twice the intensity of the upper band and most likely represents the CA1 and CA3 doublet.

The N termini of *F. pringlei* CA1 and CA3 have characteristics of chloroplast transit peptides, including an enrichment of Ser and Thr residues and a relatively low number of acidic amino acids (von Heijne et al., 1989). The results of protein targeting and localization prediction programs (Emanuelsson et al., 1999, 2000; Bannai et al., 2002; Small et al., 2004; Horton et al., 2007) also suggested that CA1 and CA3 are targeted to the chloroplast stroma. Indeed, using the anti-*F. bidentis* CA3 antiserum to label *F. pringlei* leaf sections, we detected CA in the chloroplasts of mesophyll cells. Unequivocal evidence for a chloroplast location of *F. pringlei* CA1 and CA3 was obtained through in vitro import assays. CA1 and CA3 precursor polypeptides were imported into isolated pea chloroplasts, and concomitant with import was processing of the CA1 and CA3 precursors to lower molecular mass polypeptides, which were protected from externally added protease.

### The C<sub>3</sub> Chloroplastic CA3 Was the Evolutionary Template for the C<sub>4</sub> Cytosolic CA3

Work with other C<sub>4</sub> photosynthetic enzymes from C<sub>3</sub> and C<sub>4</sub> *Flaveria* species has shown that alterations in gene expression patterns occurred during the evolution of the C<sub>4</sub> forms of the enzymes, which have resulted in their increased levels of expression and cell- and organ-specific expression patterns (Marshall et al., 1996; Drincovich et al., 1998; Rosche et al., 1998; Lai et al., 2002; Gowik et al., 2004). Similar modifications are anticipated to have occurred during the evolution of the gene encoding the C<sub>4</sub> form of  $\beta$ -CA. In addition, changes in protein targeting signals likely evolved, because in contrast to C<sub>3</sub> plants (Poincelot, 1972; Jacobson et al., 1975; Tsuzuki et al., 1985), CA activity is significantly less in C<sub>4</sub> chloroplasts and much higher in the C<sub>4</sub> mesophyll cytosol (Gutierrez et al., 1974).

We have identified orthologs of *F. pringlei* CA1, CA2, and CA3 in the C<sub>4</sub> *Flaveria* species, *F. bidentis* (Cavallaro et al., 1994; Ludwig and Burnell, 1995; Tetu et al., 2007). *F. bidentis* CA1 and CA2 show 97% and 93% sequence identity with the corresponding *F. pringlei* proteins,

and like the *F. pringlei* proteins, they localize to the chloroplast and cytosol, respectively (Tetu et al., 2007). In contrast, *F. bidentis* CA3 is a cytosolic isoform, while *F. pringlei* CA3 is a chloroplastic enzyme. We have shown that *F. bidentis* CA3 is the  $\beta$ -CA isoform providing bicarbonate for PEPC in the cytosol of mesophyll cells, that this isoform is expressed at high levels in leaves, and that this high level of expression is required for the proper functioning of the C<sub>4</sub> photosynthetic pathway in *F. bidentis* (von Caemmerer et al., 2004; Tetu et al., 2007).

Comparison of the deduced amino acid sequences of *F. bidentis* and *F. pringlei* CA3 cDNAs shows that the initiating Met of *F. bidentis* CA3 aligns with Met-72 of *F. pringlei* CA3, which is just C terminal to the region of the *F. pringlei* protein that shows similarities to a chloroplast transit peptide (Fig. 1). The two sequences are 93% identical over this shared region, with nearly half of the differences being conserved amino acid changes. From the results presented here and previously (Tetu et al., 2007), we suggest that a duplication event occurred in the ancestor of C<sub>3</sub> *Flaveria* species such that two copies of the gene encoding chloroplastic  $\beta$ -CA resulted (e.g. CA1 and CA3). Subsequently, during the evolution of C<sub>4</sub> *Flaveria* species from their C<sub>3</sub> ancestors, neofunctionalization of the CA3 gene occurred, and this involved mutations that resulted in the loss of the nucleotides encoding the chloroplast transit peptide. The consequence of this loss was the retention and operation of the CA3 protein in the C<sub>4</sub> mesophyll cytosol.

Other mutation(s) in the CA3 gene during the evolution of C<sub>4</sub> *Flaveria* species resulted in the up-regulation of its expression. A cis-regulatory element, the mesophyll expression module 1 (*Mem1*), has been identified in the upstream region of the *Flaveria* C<sub>4</sub> PEPC gene and was shown to be responsible for its high mesophyll-specific expression (Gowik et al., 2004). We have identified a *Mem1*-like element in the upstream region of the *F. bidentis* CA3 gene (data not shown), and work is continuing to determine if it directs high levels of expression of this gene in the C<sub>4</sub> mesophyll.

### Plastidial CA Isoforms Have Multiple Functions

Current opinion regarding the function of  $\beta$ -CA in C<sub>3</sub> chloroplasts is that the enzyme facilitates the diffusion of CO<sub>2</sub> into the organelle, ensuring that adequate supplies of CO<sub>2</sub> are available for Rubisco carboxylase activity (Reed and Graham, 1981; Cowan, 1986; Price et al., 1994). Modeling studies (Cowan, 1986), a decrease in carbon isotope discrimination in transgenic tobacco (*Nicotiana tabacum*) plants with severely reduced CA activity (Price et al., 1994; Williams et al., 1996), the coelution of  $\beta$ -CA and Rubisco, along with other enzymes of the photosynthetic carbon reduction cycle, in multienzyme complexes (Jebanathirajah and Coleman, 1998), and the colocalization of  $\beta$ -CA and Rubisco in sections of pea chloroplasts

(Anderson and Carol, 2004) are consistent with this hypothesis. The lack of a significant effect on CO<sub>2</sub> assimilation when CA activity was reduced using antisense and gene knockout technologies (Majeau et al., 1994; Price et al., 1994; Ferreira et al., 2008), except during early seedling development in *Arabidopsis* (Ferreira et al., 2008), however, argues against chloroplastic  $\beta$ -CA in C<sub>3</sub> plants having a major role in photosynthesis.

A number of studies have provided evidence indicating nonphotosynthetic roles for plastidial  $\beta$ -CAs, including involvement in lipogenesis in both photosynthetic and nonphotosynthetic tissues by supplying bicarbonate to acetyl-CoA carboxylase (Hoang et al., 1999; Hoang and Chapman, 2002) and in plant defense by acting as a salicylic acid-binding protein (Slaymaker et al., 2002). Wang et al. (2009) have suggested that these two roles may be linked, as evidence exists for plant defense pathways being regulated by lipid-based signals (Nandi et al., 2004; Chandra-Shekara et al., 2007).

Our results are consistent with these multiple roles of plastidial  $\beta$ -CA(s). *CA1* and *CA3* transcripts were at least 10 times more abundant than those of the *CA2* gene in *F. pringlei* mature leaves. Furthermore, because *CA3* mRNA was below detection in *F. pringlei* roots and flowers and *CA1* transcripts were measurable in both organs, albeit at lower levels than *CA2* transcripts, it is not unreasonable to suggest that *CA3* may be the isoform involved in CO<sub>2</sub> assimilation whereas *CA1* may carry out nonphotosynthetic functions, such as antioxidant activity and providing carbon for fatty acid synthesis. We have recently suggested that *CA1* in the C<sub>4</sub> *F. bidentis* (Tetu et al., 2007) carries out the same role(s); consequently, the ancestral C<sub>3</sub> function of *CA1* has been maintained in the C<sub>4</sub> *Flaveria*.

*Arabidopsis* also contains two chloroplastic  $\beta$ -CAs; however, unlike the nearly equal steady-state levels of *F. pringlei CA1* and *CA3* transcripts, *AtβCA1* signatures from massively parallel signature sequencing (Nakano et al., 2006) are 25 to 100 times higher than *AtβCA5* signatures in leaves (<http://mpss.udel.edu/at/>). This disparity holds at the protein level, with quantification of the stromal proteome demonstrating that *AtβCA1* is at least 2 orders of magnitude more abundant than *AtβCA5* (Zybailov et al., 2008). In roots, *AtβCA5* transcripts are 10 times more abundant than those of *AtβCA1* (<http://mpss.udel.edu/at/>). The ability of two  $\beta$ -CAs to function in different pathways in the same intracellular compartment may be accommodated by differing biochemical and physicochemical properties and/or the organization of the isoforms into distinct macromolecular complexes and metabolic channeling (Winkel, 2004). Examination of these characteristics may resolve the functions of plastidial  $\beta$ -CAs in both C<sub>3</sub> and C<sub>4</sub> plants, and experiments are ongoing.

### *F. pringlei CA2* Encodes a Cytosolic Enzyme

Our immunolabeling studies of *F. pringlei* leaf sections indicated that a cytosolic  $\beta$ -CA, as well as chloroplastic forms of the enzyme, are present in this C<sub>3</sub> species. Strong support for the existence of a cytosolic  $\beta$ -CA in *F. pringlei* came from in vitro import assays that showed that no processed form of *CA2* was detected in isolated chloroplasts under conditions favoring import, and the *CA2* precursor polypeptide was susceptible to digestion by externally added thermolysin. These results were also in agreement with subcellular prediction programs, which calculated *F. pringlei CA2* to be a cytosolic protein.

One function of C<sub>3</sub> cytosolic  $\beta$ -CAs is likely to be the provision of bicarbonate to PEPC, which is involved in generating carbon skeletons for amino acid synthesis and replenishment of Krebs cycle intermediates (Fett and Coleman, 1994; Raven and Newman, 1994; Chollet et al., 1996). This PEPC activity would occur in both photosynthetic and nongreen tissues. Transcripts encoding the two *Arabidopsis* cytosolic CAs, *AtβCA2* and *AtβCA3*, were found in leaves and roots (Fabre et al., 2007), although *AtβCA3* was not detected in several *Arabidopsis* leaf proteome studies (Giavalisco et al., 2005; Bindschedler et al., 2008; Rutschow et al., 2008). Under sulfur-limiting conditions, *AtβCA3* showed increased expression in roots, leading to the suggestion that *AtβCA3* specifically provides PEPC with bicarbonate for elevated respiratory activity under oxidative stress (Maruyama-Nakashita et al., 2003).

Results of our qRT-PCR assays are consistent with *F. pringlei CA2* providing bicarbonate for PEPC in green and nongreen tissues. *CA2* is expressed in leaves, and although overall  $\beta$ -CA gene expression levels were comparatively low in the nonphotosynthetic tissues we examined, *CA2* transcripts were at least 1 order and 2 orders of magnitude more abundant than *CA1* and *CA3* transcripts in flowers and roots, respectively. *F. pringlei CA2* shows 93% sequence identity with the corresponding *F. bidentis* protein, which also localizes to the cytosol (Tetu et al., 2007). Transcripts encoding the *F. bidentis CA2* isoform, like *F. pringlei CA2* mRNA,

**Table II.** *F. pringlei*  $\beta$ -CA gene-specific primers used in this study

Primer Name	Sequence (5'–3')
CA1 5' RACE	GGAGCTTTGGTGTGCGGGTGCTGCGG
CA2 5' RACE	TTAAACTCACCGCGTCTGACACCTCC
CA3 5' RACE	GGTCAAATCCGGGTTTGGTACTGTCAAG
CA1 3' RACE	CGAATTGGACCGAAGATGGAAATG
CA2 3' RACE	CGCCGAGAAGATCAAACAGCTCACC
CA3 3' RACE	CACCGCCCACTTCAAACACTTG
CA1 qRT-PCR <sup>a</sup>	CCCAGACGAAGGACCTCACTC
CA1 qRT-PCR <sup>b</sup>	AGACGAAAGGCCAAAGTCAAGTG
CA2 qRT-PCR <sup>a</sup>	AGTACTCGGATCTATGCACCAAG
CA2 qRT-PCR <sup>b</sup>	GGGTGATGAGTGAAAGTTCATTAG
CA3 qRT-PCR <sup>a</sup>	ATCACTTGATGATCAATGTGTATCC
CA3 qRT-PCR <sup>b</sup>	GTAATGATGTAATTGTACAAAAGTAAC

<sup>a</sup>F denotes forward primers. <sup>b</sup>R denotes reverse primers.

were found in all organs examined, supporting the hypothesis that this enzyme is involved in anaplerotic functions. Accordingly, it appears that, as for CA1, CA2 has retained its ancestral C<sub>3</sub> role in C<sub>4</sub> plants.

Interestingly, cytosolic  $\beta$ -CAs have been found associated with the plasma membranes of several plant species (Utsunomiya and Muto, 1993; Santoni et al., 1998; Kawamura and Uemura, 2003; Alexandersson et al., 2004; Mongrand et al., 2004; Benschop et al., 2007; Mitra et al., 2007), and At $\beta$ CA4 specifically localizes to Arabidopsis cell membranes (Fabre et al., 2007). Mongrand et al. (2004) showed that tobacco plasma membrane lipid rafts were enriched in a cytosolic  $\beta$ -CA and an aquaporin, NtAQP1, which has CO<sub>2</sub> transport activity (Uehlein et al., 2003) and decreases the resistance of the envelope to CO<sub>2</sub> (Uehlein et al., 2008).  $\beta$ -CA has also been implicated as a factor aiding the conductance of CO<sub>2</sub> through the leaf (Cowan, 1986). Whether cytosolic, membrane-associated, and/or plastidial  $\beta$ -CA isoforms function along with aquaporins to facilitate CO<sub>2</sub> transport across cell membranes to the sites of carboxylation in the chloroplast is currently being considered.

## MATERIALS AND METHODS

### Plant Material

*Flaveria pringlei* plants were grown from seeds or cuttings throughout the year in a naturally illuminated glasshouse with mean temperatures of 26°C/20°C (day/night). Plants were fertilized with a slow-release fertilizer, which was replenished every 6 months. Freshly harvested leaves were used for immunocytochemistry. For all other experiments, tissues were harvested, immediately frozen in liquid nitrogen, and stored at -80°C until use. The source of the *F. pringlei* plants was seeds collected on June 7, 1984, in Oaxaca, Mexico, near the pass between Tamazulapán and Yanhuitlán, Highway 130 (voucher specimen Jones and Jones 187).

Pea (*Pisum sativum* 'Green Feast') plants were grown for in vitro import assays as described by Tetu et al. (2007).

### *F. pringlei* Leaf $\beta$ -CA cDNAs

Total RNA was isolated from approximately 80 mg of *F. pringlei* leaves (Perfect RNA Mini Kit; Eppendorf), and the poly(A)<sup>+</sup> RNA fraction was collected using Dynal oligo(dT)<sub>25</sub>-conjugated paramagnetic beads (Merck). An adaptor-ligated leaf cDNA library was constructed using 1  $\mu$ g of poly(A)<sup>+</sup> RNA and the Marathon cDNA Amplification Kit (Clontech) and then used to isolate cDNAs encoding  $\beta$ -CA in RACE PCRs. RACE reactions consisted of 400 nM AP1 or AP2 primer (Clontech), 400 nM gene-specific primer (Table II; 5' and 3' RACE CA1-3 primers), 200  $\mu$ M dATP, dCTP, dGTP, and dTTP, 1 $\times$  High Fidelity buffer (Eppendorf), 0.5 unit of Triple Master enzyme mix (Eppendorf), and 0.1 volume of the *F. pringlei* leaf cDNA library. Amplification was done using the following conditions: 95°C for 10 min; five cycles at 95°C for 5 s, 72°C for 3 min; five cycles at 95°C for 5 s, 70°C for 3 min; and 25 cycles at 95°C for 5 s, 68°C for 3 min. Sequences of the amplification products were determined (BigDye Terminator version 3.1 Cycle Sequencing Kit; Applied Biosystems) and analyzed using MacVector 9.0 (Accelrys).

### Genomic Southern-Blot Analysis

Genomic DNA was isolated from leaf tissue according to the method of Marshall et al. (1996), and 10- $\mu$ g aliquots were digested to completion in separate reactions with *Eco*RI and *Xba*I. Genomic DNA fragments were separated by electrophoresis on a 0.8% (w/v) agarose gel and transferred to Hybond N<sup>+</sup> membranes (GE Healthcare Life Sciences) using alkaline capillary blotting

(Sambrook et al., 1989). A hybridization probe, targeting a conserved region in the *F. pringlei* CA1, CA2, and CA3 nucleotide sequences, was derived by digestion of *F. pringlei* CA2 cDNA with *Hind*III. The resulting 633-bp fragment was labeled with [ $\alpha$ -<sup>32</sup>P]dATP (DECAprime II; Ambion). Prehybridization, hybridization, and wash steps were done as described by Tetu et al. (2007).

### qRT-PCR Assays

Total RNA was isolated (Perfect RNA Mini Kit; Eppendorf) in duplicate from 80 to 150 mg of leaves, roots, and flowers from three individual *F. pringlei* plants (plants I, II, and III), and genomic DNA in the samples was removed by digestion with RQ1 RNase-free DNase (Promega) according to the supplier's instructions. cDNA was synthesized using 1  $\mu$ g of DNase-treated RNA and 20 units of Moloney murine leukemia virus reverse transcriptase (RNase H Minus; Promega) in 1 $\times$  reverse transcriptase buffer (Promega) containing 1 mM dATP, dCTP, dGTP, and dTTP, 2.5  $\mu$ M oligo(dT)<sub>15</sub> primer, 5 mM dithiothreitol, and 20 units of RNase inhibitor (RNasin Ribonuclease Inhibitor; Promega). The cDNA was stored in aliquots at -20°C to reduce degradation from repeated freeze-thaw cycles.

A standard template for qRT-PCR was constructed by inserting regions just upstream of the stop codon (CA1) or flanking the stop codon (CA2 and CA3) in tandem into pGEM-T (Promega). These regions share little nucleic acid sequence homology, which facilitated the design of CA gene-specific primers (Table II, qRT-PCR primers). Using these primers, fragments of 280, 214, and 230 bp were amplified from CA1, CA2, and CA3 targets, respectively. A standard curve was generated for each of the three CA targets using SYBR Green fluorescence (QuantiTect SYBR Green PCR Kit; Qiagen) and the PCR conditions described below with 10-fold serial dilutions of the standard template, after it was linearized by digestion with *Pst*I. The standard curves had regression coefficients of -1.00, mean squared errors of 15% or less, and slopes between -3.2 and -3.9. A slope of -3.32 indicates the PCR is 100% efficient, and deviations from 100% efficiency were calculated by the following equation: PCR efficiency = 10<sup>-1/slope</sup> - 1 (Ginzinger, 2002).

Quantification of CA1, CA2, and CA3 gene transcripts in *F. pringlei* organs was done using the LightCycler (Roche) and SYBR Green fluorescence (Qiagen). The qRT-PCR conditions were optimized to an annealing temperature of 62°C, gene-specific primer (Table II, qRT-PCR primers) concentrations of 0.2  $\mu$ M, and final Mg<sup>2+</sup> concentrations of 3.5 mM for CA1 and CA2 amplification and 5.5 mM for the amplification of CA3 targets. The cycling conditions were as follows: 95°C for 15 min; 95°C for 15 s, 62°C for 30 s, 72°C for 30 s (40 cycles); and single data acquisition. The levels of CA transcripts were calculated using the LightCycler Data Analysis Software version 3.5 (Roche). Melt curve analysis was routinely done following the supplier's instructions (Roche). Amplification products were visualized on ethidium bromide-stained agarose gels to verify the specificity of the products and to correlate product length with melting peaks.

As at least three qRT-PCRs were carried out for each of the duplicate cDNA preparations, separate ANOVA (SPSS software) tests were used to examine the variation in transcript abundances between organs with cDNA preparations from the same and from different plants. One-way ANOVA indicated that the CA genes showed significant differences in expression among the organ samples ( $P < 0.05$ ; data not shown). Similarly, ANOVA demonstrated that distinct cDNA pools from a particular organ of different plants contained significantly different amounts of transcript encoding each CA isoform ( $P < 0.05$ ; data not shown), whereas ANOVAs comparing duplicate cDNA pools from a particular organ of the same plant showed no significant variation ( $P > 0.05$ ; data not shown). Thus, this statistical analysis demonstrated that data obtained from the duplicate cDNA pools from a particular organ of the same plant could be combined, whereas data obtained from cDNA pools of a particular organ from different plants could not be combined. Therefore, the results shown represent mean CA transcript concentrations for each plant organ using values obtained from the same plant.

### Chloroplast Import Assays

Individual plasmids (0.5–1  $\mu$ g) containing inserts encoding the ORFs of *F. pringlei* CA1, CA2, or CA3 and pea Rubisco SSU were used to synthesize precursor proteins in the presence of [<sup>35</sup>S]Met in a coupled transcription/translation rabbit reticulocyte lysate system (T<sub>N</sub>T; Promega) according to the manufacturer's instructions. The isolation of intact pea chloroplasts and in vitro import assays were done as described previously (Tetu et al., 2007).

## Immunodetection Methods

An anti-*Flaveria bidentis* CA3 affinity-purified antiserum was used to detect  $\beta$ -CA polypeptides on immunoblots of *F. pringlei* soluble leaf proteins and on *F. pringlei* leaf sections as described by Tetu et al. (2007).

## Phylogenetic Analysis

Sequences encoding  $\beta$ -CA were retrieved using genomes identified in GenBank (www.ncbi.nlm.nih.gov) and Phytozome (www.phytozome.net) databases for which there is complete sequence information. BLASTP (Altschul et al., 1990) was used with *Arabidopsis thaliana* At $\beta$ CA1 and At $\beta$ CA6 (Fabre et al., 2007) to query the genomes. To recover additional related  $\beta$ -CA sequences, each species-specific sequence retrieved was then used to query GenBank and species-specific databases using BLASTP and TBLASTN (Altschul et al., 1990). Sequences were aligned with ClustalW (Thompson et al., 1994), and N and C termini were trimmed to remove noninformative residues, such as targeting sequences. This resulted in core  $\beta$ -CA sequences of approximately 200 amino acids containing the residues required for catalysis and secondary structure (Kimber and Pai, 2000). Redundant CA sequences were removed from the alignment, and the phylogeny of the remaining sequences was reconstructed using the neighbor-joining method (Saitou and Nei, 1987) included in the MacVector 9.0 Sequence Analysis Software (Accelrys). Roman numerals were arbitrarily assigned to the  $\beta$ -CA sequences from a species to facilitate analyses; they do not imply relatedness or functional similarities of  $\beta$ -CA isoforms between species.

Accession numbers for the sequences used in the analysis are as follows: *Arabidopsis* CA1 to CA6 (Fabre et al., 2007); *F. bidentis* CA1 to CA3 (Tetu et al., 2007); *F. pringlei* CA1 to CA3 (GenBank accession nos. P46281, DQ273586, and DQ273587, respectively); *Glycine max* CAI and CAII (GenBank accession nos. AK243989 and AK287413, respectively); *Medicago truncatula* CAI to CAIV (MTpep2 Database [International *Medicago* Genome Annotation Group] nos. AC124951\_31.5, CU302343\_11.3, AC157505\_3.5, and CU179920\_2.3, respectively); *Oryza sativa* subsp. *japonica* CAI and CAII (GenBank accession nos. Os01g063990 and Os09g0464000, respectively); *Physcomitrella patens* CAI to CAV (Phytozome DBXREF nos. 123406, 130288, 147703, 205864, and 162454, respectively); *Populus trichocarpa* CAI to CAVI (*Populus* genome release 1.1 [Department of Energy Joint Genome Institute] identifiers estEXT\_Genewise, estEXT\_fgenesh, gw1.VIII.1764.1, eug3.00150550, gw1.XVII.194.1, and gw1.V4618.1, respectively); *Selaginella moellendorffii* CAI to CAVI (Phytozome DBXREF nos. 102513, 81873, 95906, 86779, 80889, and 25779, respectively); *Sorghum bicolor* CAI to CAIII (Phytozome DBXREF nos. Sb02g026930, Sb03g029180, and Sb03g029190, respectively); *Vitis vinifera* CAI to CAV (Phytozome DBXREF nos. GSVIVT00020732001, GSVIVT00016080001, GSVIVT00016078001, GSVIVT00015113001, and GSVIVT00007538001, respectively); and *Zea mays* CAI to CAIV (GenBank accession nos. ACF78806, ACF88455, ACF82348, and ACF86418, respectively).

## ACKNOWLEDGMENTS

We thank Jim Whelan for the pea Rubisco SSU clone. We are also grateful to Debra Birch and Nancy Hancock for excellent technical support. The generous assistance of Michael Powell, Scott Holaday, Stanley Jones, and Peter Westhoff regarding the collection details of the *F. pringlei* seed source is greatly appreciated, as was the information provided by Monique Reed, Dale Kruse, and Tom Wendt.

Received February 21, 2009; accepted May 11, 2009; published May 15, 2009.

## LITERATURE CITED

- Alexandersson E, Saalbach G, Larsson C, Kjellbom P (2004) *Arabidopsis* plasma membrane proteomics identifies components of transport, signal transduction and membrane trafficking. *Plant Cell Physiol* **45**: 1543–1556
- Altschul SE, Gish W, Miller W, Myers EW, Lipman DJ (1990) Basic local alignment search tool. *J Mol Biol* **215**: 403–410
- Anderson LE, Carol AA (2004) Enzyme co-localization with Rubisco in pea leaf chloroplasts. *Photosynth Res* **82**: 49–58
- Arabidopsis Genome Initiative (2000) Analysis of the genome sequence of the flowering plant *Arabidopsis thaliana*. *Nature* **408**: 796–815

- Bannai H, Tamada Y, Maruyama O, Nakai K, Miyano S (2002) Extensive feature detection of N-terminal protein sorting signals. *Bioinformatics* **18**: 298–305
- Benschop JJ, Mohammed S, O'Flaherty M, Heck AJR, Slijper M, Menke FLH (2007) Quantitative phosphoproteomics of early elicitor signaling in *Arabidopsis*. *Mol Cell Proteomics* **6**: 1198–1214
- Bindschedler LV, Palmblad M, Cramer R (2008) Hydroponic isotope labelling of entire plants (HILEP) for quantitative plant proteomics: an oxidative stress case study. *Phytochemistry* **69**: 1962–1972
- Bracey MH, Christiansen J, Tovar P, Cramer SP, Bartlett SG (1994) Spinach carbonic anhydrase: investigation of the zinc-binding ligands by site-directed mutagenesis, elemental analysis, and EXAFS. *Biochemistry* **33**: 13126–13131
- Burnell JN, Gibbs MJ, Mason JG (1990) Spinach chloroplastic carbonic anhydrase: nucleotide sequence analysis of cDNA. *Plant Physiol* **92**: 37–40
- Cavallaro A, Ludwig M, Burnell J (1994) The nucleotide sequence of a complementary DNA encoding *Flaveria bidentis* carbonic anhydrase. *FEBS Lett* **350**: 216–218
- Chandra-Shekara AC, Venugopal SC, Barman SR, Kachroo A, Kachroo P (2007) Plastidial fatty acid levels regulate resistance gene-dependent defense signaling in *Arabidopsis*. *Proc Natl Acad Sci USA* **104**: 7277–7282
- Chollet R, Vidal J, O'Leary MH (1996) Phosphoenolpyruvate carboxylase: a ubiquitous, highly regulated enzyme in plants. *Annu Rev Plant Physiol Plant Mol Biol* **47**: 273–298
- Christin PA, Besnard G, Samaritani E, Duvall MR, Hodkinson TR, Savolainen V, Salamin N (2008) Oligocene CO<sub>2</sub> decline promoted C<sub>4</sub> photosynthesis in grasses. *Curr Biol* **18**: 37–43
- Cowan IR (1986) Economics of carbon fixation in higher plants. In TJ Givnish, ed, *On the Economy of Plant Form and Function*. Cambridge University Press, Cambridge, UK, pp 133–170
- Dean C, Tamaki S, Dunsmuir P, Favreau M, Katayama C, Dooner H, Bedbrook J (1986) mRNA transcripts of several plant genes are polyadenylated at multiple sites in vivo. *Nucleic Acids Res* **14**: 2229–2240
- Drincovich ME, Casati P, Andreo CS, Chessin SJ, Franceschi VR, Edwards GE, Ku MSB (1998) Evolution of C<sub>4</sub> photosynthesis in *Flaveria* species: isoforms of NADP-malic enzyme. *Plant Physiol* **117**: 733–744
- Ehleringer JR, Monson RK (1993) Evolutionary and ecological aspects of photosynthetic pathway variation. *Annu Rev Ecol Syst* **24**: 411–439
- Emanuelsson O, Nielsen H, Brunak S, von Heijne G (2000) Predicting subcellular localization of proteins based on their N-terminal amino acid sequence. *J Mol Biol* **300**: 1005–1016
- Emanuelsson O, Nielsen H, von Heijne G (1999) ChloroP, a neural network-based method for predicting chloroplast transit peptides and their cleavage sites. *Protein Sci* **8**: 978–984
- Fabre N, Reiter IM, Becuwe-Linka N, Genty B, Rumeau D (2007) Characterization and expression analysis of genes encoding  $\alpha$  and  $\beta$  carbonic anhydrases in *Arabidopsis*. *Plant Cell Environ* **30**: 617–629
- Ferreira FJ, Guo C, Coleman JR (2008) Reduction of plastid-localized carbonic anhydrase activity results in reduced *Arabidopsis* seedling survivorship. *Plant Physiol* **147**: 585–594
- Fett JP, Coleman JR (1994) Characterization and expression of two cDNAs encoding carbonic anhydrase in *Arabidopsis thaliana*. *Plant Physiol* **105**: 707–713
- Giaivalisco P, Nordhoff E, Kreitler T, Klöppel KD, Lehrach H, Klose J, Gobom J (2005) Proteome analysis of *Arabidopsis thaliana* by two-dimensional gel electrophoresis and matrix-assisted laser desorption/ionisation-time-of-flight mass spectrometry. *Proteomics* **5**: 1902–1913
- Ginzinger DG (2002) Gene quantification using real-time quantitative PCR: an emerging technology hits the mainstream. *Exp Hematol* **30**: 503–512
- Gowik U, Burscheidt J, Akyildiz M, Schlue U, Koczor M, Streubel M, Westhoff P (2004) *cis*-Regulatory elements for mesophyll-specific gene expression in the C<sub>4</sub> plant *Flaveria trinervia*, the promoter of the C<sub>4</sub> phosphoenolpyruvate carboxylase gene. *Plant Cell* **16**: 1077–1090
- Gowik U, Engelmann S, Bläsing OE, Raghavendra AS, Westhoff P (2006) Evolution of C<sub>4</sub> phosphoenolpyruvate carboxylase in the genus *Alternanthera*: gene families and the enzymatic characteristics of the C<sub>4</sub> isozyme and its orthologues in C<sub>3</sub> and C<sub>3</sub>/C<sub>4</sub> *Alternanthera*. *Planta* **223**: 359–368
- Gutiérrez M, Huber SC, Ku SB, Kanai R, Edwards GE (1974) Intracellular localization of carbon metabolism in mesophyll cells of C<sub>4</sub> plants. In M Avron, ed, *Proceedings of the Third International Congress on Photosynthesis*. Elsevier Science Publishers, Amsterdam, pp 1219–1230

- Gygi SP, Rochon Y, Franza BR, Aebersold R (1999) Correlation between protein and mRNA abundance in yeast. *Mol Cell Biol* **19**: 1720–1730
- Hatch MD (1987) C<sub>4</sub> photosynthesis: a unique blend of modified biochemistry, anatomy and ultrastructure. *Biochim Biophys Acta* **895**: 81–106
- Hatch MD, Burnell JN (1990) Carbonic anhydrase activity in leaves and its role in the first step of C<sub>4</sub> photosynthesis. *Plant Physiol* **93**: 825–828
- Hermans J, Westhoff P (1990) Analysis of expression and evolutionary relationships of phosphoenolpyruvate carboxylase genes in *Flaveria trinervia* (C<sub>4</sub>) and *F. pringlei* (C<sub>3</sub>). *Mol Gen Genet* **224**: 459–468
- Hoang CV, Chapman KD (2002) Biochemical and molecular inhibition of plastidial carbonic anhydrase reduces the incorporation of acetate into lipids in cotton embryos and tobacco cell suspensions and leaves. *Plant Physiol* **128**: 1417–1427
- Hoang CV, Wessler HG, Local A, Turley RB, Benjamin RC, Chapman KD (1999) Identification and expression of cotton (*Gossypium hirsutum* L.) plastidial carbonic anhydrase. *Plant Cell Physiol* **40**: 1262–1270
- Horton P, Park KJ, Obayashi T, Fujita N, Harada H, Adams-Collier CJ, Nakai K (2007) WoLF PSORT: protein localization predictor. *Nucleic Acids Res* **35**: W585–W587
- Imaizumi N, Ku MSB, Ishihara K, Samejima M, Kaneko S, Matsuoka M (1997) Characterization of the gene for pyruvate, orthophosphate dikinase from rice, a C<sub>3</sub> plant, and a comparison of structure and expression between C<sub>3</sub> and C<sub>4</sub> genes for this protein. *Plant Mol Biol* **34**: 701–716
- Jacobson BS, Fong E, Heath RL (1975) Carbonic anhydrase of spinach: studies on its location, inhibition, and physiological function. *Plant Physiol* **55**: 468–474
- Jebanathirajah JA, Coleman JR (1998) Association of carbonic anhydrase with a Calvin cycle enzyme complex in *Nicotiana tabacum*. *Planta* **204**: 177–182
- Jenkins CLD, Furbank RT, Hatch MD (1989) Mechanism of C<sub>4</sub> photosynthesis: a model describing the inorganic carbon pool in bundle sheath cells. *Plant Physiol* **91**: 1372–1381
- Kawamura T, Shigesada K, Toh H, Okumura S, Yanagisawa S, Izui K (1992) Molecular evolution of phosphoenolpyruvate carboxylase for C<sub>4</sub> photosynthesis in maize: comparison of its cDNA sequence with a newly isolated cDNA encoding an isozyme involved in the anaplerotic function. *J Biochem* **112**: 147–154
- Kawamura Y, Uemura M (2003) Mass spectrometric approach for identifying putative plasma membrane proteins of *Arabidopsis* leaves associated with cold acclimation. *Plant J* **36**: 141–154
- Kimber MS, Pai EF (2000) The active site architecture of *Pisum sativum*  $\beta$ -carbonic anhydrase is a mirror image of that of  $\alpha$ -carbonic anhydrases. *EMBO J* **19**: 1407–1418
- Lai LB, Wang L, Nelson TM (2002) Distinct but conserved functions for two chloroplastic NADP-malic enzyme isoforms in C<sub>3</sub> and C<sub>4</sub> *Flaveria* species. *Plant Physiol* **128**: 125–139
- Long SP (1999) Environmental responses. In RF Sage, RK Monson, eds, C<sub>4</sub> Plant Biology. Academic Press, San Diego, pp 215–249
- Ludwig M, Burnell JN (1995) Molecular comparison of carbonic anhydrase from *Flaveria* species demonstrating different photosynthetic pathways. *Plant Mol Biol* **29**: 353–365
- Majeau N, Arnoldo M, Coleman JR (1994) Modification of carbonic anhydrase activity by antisense and over-expression constructs in transgenic tobacco. *Plant Mol Biol* **25**: 377–385
- Marshall JS, Stubbs JD, Taylor WC (1996) Two genes encode highly similar chloroplastic NADP-malic enzymes in *Flaveria*: implications for the evolution of C<sub>4</sub> photosynthesis. *Plant Physiol* **111**: 1251–1261
- Maruyama-Nakashita A, Inoue E, Watanabe-Takahashi A, Yamaya T, Takahashi H (2003) Transcriptome profiling of sulfur-responsive genes in *Arabidopsis* reveals global effects of sulfur nutrition on multiple metabolic pathways. *Plant Physiol* **132**: 597–605
- McKown AD, Moncalvo JM, Dengler NG (2005) Phylogeny of *Flaveria* (Asteraceae) and inference of C<sub>4</sub> photosynthesis evolution. *Am J Bot* **92**: 1911–1928
- Mitra SK, Gantt JA, Ruby JE, Clouse SD, Goshe MB (2007) Membrane proteomic analysis of *Arabidopsis thaliana* using alternative solubilization techniques. *J Proteome Res* **6**: 1933–1950
- Mongrand S, Morel J, Laroche J, Claverol S, Carde JP, Hartmann MA, Bonneau M, Simon-Plas F, Lessire R, Bessoule JJ (2004) Lipid rafts in higher plant cells. *J Biol Chem* **279**: 36277–36286
- Monson RK (2003) Gene duplication, neofunctionalization, and the evolution of C<sub>4</sub> photosynthesis. *Int J Plant Sci* **164**: S43–S54
- Nakano M, Nobuta K, Vemaraju K, Tej SS, Skogen JW, Meyers BC (2006) Plant MPSS databases: signature-based transcriptional resources for analyses of mRNA and small RNA. *Nucleic Acids Res* **34**: D731–D735
- Nandi A, Weltri R, Shah J (2004) The *Arabidopsis thaliana* dihydroxyacetone phosphate reductase gene *SUPPRESSOR OF FATTY ACID DESATURASE DEFICIENCY1* is required for glycerolipid metabolism and for the activation of systemic acquired resistance. *Plant Cell* **16**: 465–477
- Okabe K, Yang SY, Tsuzuki M, Miyachi S (1984) Carbonic anhydrase: its content in spinach leaves and its taxonomic diversity studied with anti-spinach leaf carbonic anhydrase antibody. *Plant Sci Lett* **33**: 145–153
- Osborne CP, Beerling DJ (2006) Nature's green revolution: the remarkable evolutionary rise of C<sub>4</sub> plants. *Philos Trans R Soc Lond B Biol Sci* **361**: 173–194
- Peltier JB, Cai Y, Sun Q, Zabrouskov V, Giacomelli L, Rudella A, Ytterberg AJ, Rutschow H, van Wijk KJ (2006) The oligomeric stromal proteome of *Arabidopsis thaliana* chloroplasts. *Mol Cell Proteomics* **5**: 114–133
- Poincelot RP (1972) Intracellular distribution of carbonic anhydrase in spinach leaves. *Biochim Biophys Acta* **258**: 637–642
- Price GD, von Caemmerer S, Evans JR, Yu JW, Lloyd J, Oja V, Kell P, Harrison K, Gallagher A, Badger MR (1994) Specific reduction of chloroplastic carbonic anhydrase activity by antisense RNA in transgenic tobacco plants has a minor effect on photosynthesis. *Planta* **193**: 331–340
- Provart NJ, Majeau N, Coleman JR (1993) Characterization of pea chloroplastic carbonic anhydrase: expression in *Escherichia coli* and site-directed mutagenesis. *Plant Mol Biol* **22**: 937–943
- Rajeevan MS, Bassett CL, Hughes DW (1991) Isolation and characterization of cDNA clones for NADP-malic enzyme from leaves of *Flaveria*: transcript abundance distinguishes C<sub>3</sub>, C<sub>3</sub>-C<sub>4</sub> and C<sub>4</sub> photosynthetic types. *Plant Mol Biol* **17**: 371–383
- Raven JA, Newman JR (1994) Requirement for carbonic anhydrase activity in processes other than photosynthetic inorganic carbon assimilation. *Plant Cell Environ* **17**: 123–130
- Reed ML, Graham D (1981) Carbonic anhydrase in plants: distribution, properties and possible physiological roles. *Prog Phytochem* **7**: 47–94
- Restrepo S, Myers KL, del Pozo O, Martin GB, Hart AL, Buell CR, Fry WE, Smart CD (2005) Gene profiling of a compatible interaction between *Phytophthora infestans* and *Solanum tuberosum* suggests a role for carbonic anhydrase. *Mol Plant Microbe Interact* **18**: 913–922
- Roeske CA, Ogren WL (1990) Nucleotide sequence of pea cDNA encoding chloroplastic carbonic anhydrase. *Nucleic Acids Res* **18**: 3413
- Rosche E, Chitty J, Westhoff P, Taylor WC (1998) Analysis of promoter activity for the gene encoding pyruvate orthophosphate dikinase in stably transformed C<sub>4</sub> *Flaveria* species. *Plant Physiol* **117**: 821–829
- Rosche E, Streubel M, Westhoff P (1994) Primary structure of the pyruvate orthophosphate dikinase of the C<sub>3</sub> plant *Flaveria pringlei* and expression analysis of pyruvate orthophosphate dikinase sequences in C<sub>3</sub>, C<sub>3</sub>-C<sub>4</sub> and C<sub>4</sub> *Flaveria* species. *Plant Mol Biol* **26**: 763–769
- Rutschow H, Ytterberg AJ, Friso G, Nilsson R, van Wijk KJ (2008) Quantitative proteomics of a chloroplast *SRP54* sorting mutant and its genetic interactions with *CLP1* in *Arabidopsis*. *Plant Physiol* **148**: 156–175
- Sage RF (2004) The evolution of C<sub>4</sub> photosynthesis. *New Phytol* **161**: 341–370
- Saitou N, Nei M (1987) The neighbor-joining method: a new method for reconstructing phylogenetic trees. *Mol Biol Evol* **4**: 406–425
- Sambrook J, Fritsch EF, Maniatis T (1989) *Molecular Cloning: A Laboratory Manual*, Ed 2. Cold Spring Harbor Laboratory Press, Cold Spring Harbor, NY
- Santoni V, Rouquié D, Dumas P, Mansion M, Boutry M, Degand H, Dupree P, Packman L, Sherrier J, Prime T, et al (1998) Use of a proteome strategy for tagging proteins present at the plasma membrane. *Plant J* **16**: 633–641
- Slaymaker DH, Navarre DA, Clark D, del Pozo O, Martin GB, Klessig DF (2002) The tobacco salicylic acid-binding protein 3 (SABP3) is the chloroplast carbonic anhydrase, which exhibits antioxidant activity and plays a role in the hypersensitive defense response. *Proc Natl Acad Sci USA* **99**: 11640–11645
- Small I, Peeters N, Legeai F, Lurin C (2004) Predotar: a tool for rapidly screening proteomes for N-terminal targeting sequences. *Proteomics* **4**: 1581–1590
- Tausta SL, Coyle HM, Rothermel B, Stiefel V, Nelson T (2002) Maize C<sub>4</sub> and non-C<sub>4</sub> NADP-dependent malic enzymes are encoded by distinct

- genes derived from a plastid-localized ancestor. *Plant Mol Biol* **50**: 635–652
- Tetu SG, Tanz SK, Vella N, Burnell JB, Ludwig M** (2007) The *Flaveria bidentis*  $\beta$ -carbonic anhydrase gene family encodes cytosolic and chloroplastic isoforms demonstrating distinct organ-specific expression patterns. *Plant Physiol* **144**: 1316–1327
- Thompson JD, Higgins DG, Gibson TJ** (1994) CLUSTAL W: improving the sensitivity of progressive multiple sequence alignment through sequence weighting, position-specific gap penalties and weight matrix choice. *Nucleic Acids Res* **22**: 4673–4680
- Tipple BJ, Pagani M** (2007) The early origins of terrestrial C<sub>4</sub> photosynthesis. *Annu Rev Earth Planet Sci* **35**: 435–461
- Tsuzuki M, Miyachi S, Edwards GE** (1985) Localization of carbonic anhydrase in mesophyll cells of terrestrial C<sub>3</sub> plants in relation to CO<sub>2</sub> assimilation. *Plant Cell Physiol* **26**: 881–891
- Uehlein N, Lovisolo C, Siefritz F, Kaldenhoff R** (2003) The tobacco aquaporin NtAQP1 is a membrane CO<sub>2</sub> pore with physiological functions. *Nature* **425**: 734–737
- Uehlein N, Otto B, Hanson DT, Fischer M, McDowell N, Kaldenhoff R** (2008) Function of *Nicotiana tabacum* aquaporins as chloroplast gas pores challenges the concept of membrane CO<sub>2</sub> permeability. *Plant Cell* **20**: 648–657
- Utsunomiya E, Muto S** (1993) Carbonic anhydrase in the plasma membranes from leaves of C<sub>3</sub> and C<sub>4</sub> plants. *Physiol Plant* **88**: 413–419
- Vicentini A, Barber JC, Aliscioni SS, Giussani LM, Kellogg EA** (2008) The age of the grasses and clusters of origins of C<sub>4</sub> photosynthesis. *Glob Change Biol* **14**: 2963–2977
- von Caemmerer S, Quinn V, Hancock N, Price GD, Furbank RT, Ludwig M** (2004) Carbonic anhydrase and C<sub>4</sub> photosynthesis: a transgenic analysis. *Plant Cell Environ* **27**: 697–703
- von Heijne G, Steppuhn J, Hermann RG** (1989) Domain structure of mitochondrial and chloroplast targeting peptides. *Eur J Biochem* **180**: 535–545
- Wang BC, Pan YH, Meng DZ, Zhu YX** (2006) Identification and quantitative analysis of significantly accumulated proteins during the *Arabidopsis* seedling de-etiolation process. *J Integr Plant Biol* **48**: 104–113
- Wang YQ, Feechan A, Yun BW, Shafiei R, Hofmann A, Taylor P, Xue P, Yang FQ, Xie ZS, Pallas JA, et al** (2009) S-Nitrosylation of AtSABP3 antagonizes the expression of plant immunity. *J Biol Chem* **284**: 2131–2137
- Williams TG, Flanagan LB, Coleman JR** (1996) Photosynthetic gas exchange and discrimination against <sup>13</sup>CO<sub>2</sub> and C<sup>18</sup>O<sup>16</sup>O in tobacco plants modified by an antisense construct to have low chloroplastic carbonic anhydrase. *Plant Physiol* **112**: 319–326
- Winkel BSJ** (2004) Metabolic channeling in plants. *Annu Rev Plant Biol* **55**: 85–107
- Zhang Z** (2003) Evolution by gene duplication. *Trends Ecol Evol* **18**: 292–298
- Zybailov B, Rutschow H, Friso G, Rudella A, Emanuelsson O, Sun Q, van Wijk KJ** (2008) Sorting signals, N-terminal modifications and abundance of the chloroplast genome. *PLoS One* **3**: e1994